Role of surfactant derived intermediates in the efficacy and mechanism for radiation chemical degradation of a hydrophobic Azo dye, 1-phenylazo-2-naphthol

ARTICLE *in* JOURNAL OF HAZARDOUS MATERIALS · MAY 2015

Impact Factor: 4.53 · DOI: 10.1016/j.jhazmat.2015.04.084

4 AUTHORS, INCLUDING:

Suchandra Chatterjee
Bhabha Atomic Research Centre
42 PUBLICATIONS **295** CITATIONS
SEE PROFILE

Soumyakanti Adhikari
Bhabha Atomic Research Centre
78 PUBLICATIONS **900** CITATIONS
SEE PROFILE

Journal of Hazardous Materials 298 (2015) 19–27

Contents lists available at ScienceDirect

Journal of Hazardous Materials

journal homepage: www.elsevier.com/locate/jhazmat

Role of surfactant derived intermediates in the efficacy and mechanism for radiation chemical degradation of a hydrophobic azo dye, 1-phenylazo-2-naphthol

Laboni Das[a], Suchandra Chatterjee[b], Devidas B. Naik[a], Soumyakanti Adhikari[a,*]

[a] Radiation & Photochemistry Division, Bhabha Atomic Research Centre, Mumbai 400085, India
[b] Food Technology Division, Bhabha Atomic Research Centre, Mumbai 400085, India

HIGHLIGHTS

- Demonstration of the role of surfactant in the degradation of the hydrophobic dye.
- First direct observation of the formation of "hydrazyl radical-parent" adduct.
- Similar products obtained in the reaction of e^-_{aq} and $^\bullet$OH radical in TX-100 medium.
- Significant reduction in cytotoxicity of irradiated dye in aqueous–organic medium.
- New mechanistic pathway could be delineated.

GRAPHICAL ABSTRACT

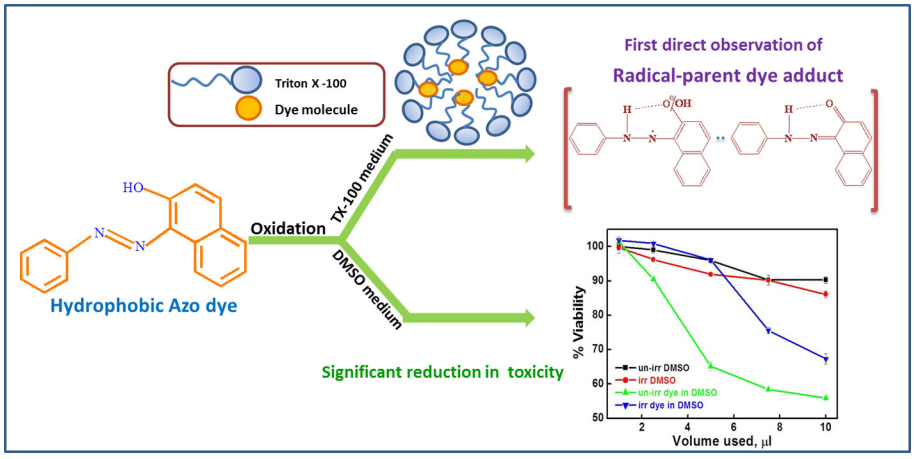

ARTICLE INFO

Article history:
Received 26 February 2015
Received in revised form 10 April 2015
Accepted 28 April 2015
Available online 6 May 2015

Keywords:
Hydrophobic azo dye
Reducing TX-100 radical
Surfactant radical induced degradation
Reduced cytotoxicity
New mechanism
Hydrazyl radical-parent adduct

ABSTRACT

A combined methodology involving gamma and pulse radiolysis, product analysis and toxicity studies has been adopted to comprehend the degradation process of a model hydrophobic azo dye, 1-phenylazo-2-naphthol, emphasizing the role of the surfactant, which is an integral part of textile waste. Two new and important findings are underlined in this article. The first is the direct attestation of the hydrazyl radical-parent adduct, formed in the reaction of the dye with e^-_{aq} followed by protonation and subsequent addition to the unreacted dye molecule. This has been confirmed from concentration dependent studies. Secondly, we have clearly shown that in the reaction of hydroxyl radical with the dye in Triton X-100 media, the initially produced TX radicals cause reductive degradation of the dye. Identification and detailed analysis of HPLC and GCMS data reveals that similar products are formed in both the reactions of e^-_{aq} and $^\bullet$OH radicals. Moreover, the cytotoxicity of 10^{-4} mol dm^{-3} dye was found to be reduced significantly after irradiation. Thus, the present study not only depicts new pathways for the degradation of hydrophobic azo dye, but also demonstrates the role of a surfactant in the entire process.

* Corresponding author. Tel.: +91 2225590301; fax: +91 2225505151.
E-mail address: asoumya@barc.gov.in (S. Adhikari).

http://dx.doi.org/10.1016/j.jhazmat.2015.04.084
0304-3894/

1. Introduction

Pre-treatment of industrial and domestic effluents containing organic compounds is necessary, which otherwise can cause serious environmental hazards. Having slow bio-degradability and generating harmful intermediates, azo dyes are one of the major concerns for waste management. In addition to their large scale use in dyestuff and textile industries, possible inclusion of azo dyes in dye-sensitized solar cells [1] is also being considered. It has been shown earlier that 1-amino 2-napthol, one of the products of bio-reductive degradation of azo dye shows very high toxicity [2]. Thus, innovative, viable and efficient treatment methods are being proposed by researchers worldwide, such as using chemical and biogenic sulphides [3], non-thermal plasma reactor [4], UV/H_2O_2 oxidation [5], Fenton process [6], photoelectrocatalytic chlorination [7], phytoremediation [8], anaerobic biodecoloration using carbonaceous materials [9] and electrochemical treatment [10] for the degradation of azo dyes. Currently, the photocatalytic processes are popularly being explored for degradation of organic dyes using graphene oxide nanocomposites [11,12]. Sonocatalysis have also shown to be a potential method for degradation of Resazurin dye [13] and Reactive Red 120 [14].

In the degradation process of azo dyes, the important points need to be addressed are; efficiency, mechanism, identification of degraded products and their toxicity. Advanced oxidation processes (AOPs) are considered to be efficient methods for the decomposition of organics including dyes [15]. Electrochemical advanced oxidation processes (EAOPs) are also showing promise for degradation of wide range of organic chemicals [16]. Fundamental aspect of AOPs is based on the generation of highly reactive oxidizing hydroxyl radicals [17]. Radiation and photochemical methods also fall under the AOPs. In the semiconductor based photocatalytic method, breakdown of water produces hydroxyl radicals, which are mainly responsible for the oxidative degradation of the organic molecules. Basic advantage of the radiation chemical method over all other AOPs is simultaneous generation of both highly reactive oxidizing and reducing radicals. This is evident as important contributions [18–26] are already available in literature highlighting the feasibility and demonstration of the use of ionizing radiation for the degradation of azo dyes. Electron beam and γ-radiation have been potentially applied in industrial scale for the degradation of environmental pollutants and other organic wastes [18,19].

In the present work, we have selected 1-phenylazo-2-napthol as a model hydrophobic azo dye, which is widely used in different industrial products including waxes, oils, petrol, polishes and coloured smoke formulations. Although the use of this dye in foods is not permitted because of its carcinogenic property [27,28],but it is still being used for colouring various foodstuffs [29], including particular brands of chilli and curry powder [30]. The tautomerism of azo dyes containing OH and azo group in neighbouring positions as shown in Fig. 1, is viewed to be an important aspect, which can be exploited for their application even in chemical sensing [31]. Below pK_a, either azo or hydrazo tautomer may dominate, depending on the substitution present in the dye. In the case of *o*-substitution to the phenyl group attached to the N═N— azo bond, the hydrazone tautomer dominates [19].

In the textile waste water, the washed out dyes, especially hydrophobic molecules are bound to the surfactants. Thus, it is rational to consider that the extent and mechanism of degradation of the dyes via AOPs would be affected by the presence of surfactants. Of late, a comparative study on simulated dye-waste-water shows that the extent of mineralization of the surfactant along with the dye is the maximum by gamma radiolysis in presence of potassium persulfate [32]. However, the role of the surfactant in the degradation mechanism is yet to be answered. With this backdrop, we have chosen Triton-X (TX-100) as a reaction medium for understanding the mechanism of radiation induced degradation of the dye, which in addition, helps in solubilisation of the dye in aqueous environment. It is also known that the non-ionic surfactants are better in solubilizing hydrophobic molecules compared to ionic counterparts [33]. This would further enable a better understanding of the role of surfactant in radiation induced degradation of the substrate incorporated inside the nonpolar core.

In the present article, gamma radiolysis method has been adopted to examine the efficiency of radical induced degradation of the dye. The pulse radiolysis technique has been utilised to understand the mechanism for the reactions of the dye with oxidizing and reducing radicals, selectively. We have demonstrated that surfactant plays very important role in the degradation process and its mechanism. Further, we propose here that, the reductive pathway becomes predominant for the degradation of the dye even in the presence of strong oxidizing primary radical, in TX-100 medium. The restricted micellar environment favours the formation of adduct between the reduced dye radical and unreacted dye molecule before giving rise to the final products. The cytotoxicity of the dye solution is found to be significantly reduced upon irradiation under oxidising condition in aqueous–organic medium.

2. Experimental

2.1. Materials

High purity chemicals, azo dye (Sudan I), *tert*-butanol, Triton-X 100, were obtained from Sigma–Aldrich and used without further purification. Other chemicals were from SD Fine-Chem. Ltd., Mumbai, with highest purity. Water used in these studies was drawn from Millipore A-10 water polishing system (resistivity of 18.2 MΩ cm^{-1} and organic carbon content <5 ppb). pH of the solutions was adjusted using NaOH and HCl solutions both at 0.1 mol dm^{-3} concentration. High purity N_2 and N_2O gases were from IOLAR. As the tested compound is insoluble in water, we have carried out the degradation experiments in minimum amount of organic solvent (34% of acetonitrile–aqueous mixture) and in 1×10^{-2} mol dm^{-3} Triton-X 100 micellar medium.

3. Methods and instrumentation

3.1. Gamma radiolysis

Samples were irradiated using GC 5000 as Co-60 γ source at a dose rate of 15 Gy/min. The decolouration curves were obtained using a JASCO V-650 absorption spectrophotometer. The degree of decolouration was calculated from the decrease in absorbance at a 485 nm wavelength (λ_{max} of the dye).

3.2. Pulse radiolysis

In pulse radiolysis, an intense pulse of electrons is used to create a non-equilibrium situation, in which significant concentration of transient species is produced in a very short time scale and these transient species are monitored by following the changes in their optical absorption. The pulse radiolysis system with 7 MeV electrons used in the present study has been described elsewhere [34]. The dosimetry was carried out using an air-saturated aqueous solution containing 5×10^{-2} mol dm^{-3} KSCN ($G\epsilon$ = 23,890 dm^3 mol^{-1} cm^{-1} per 100 eV at 500 nm) [35]. Unless otherwise mentioned, the pulse radiolysis experiments were carried out at a dose of 35 Gy/pulse. In an aqueous solution, the electron pulse from the accelerator initiates a series of rapid reactions leading to the formation of the desired radicals as follows:

$$H_2O \rightsquigarrow e^-_{aq}, H^\bullet, {}^\bullet OH, H_2, H_2O_2, H_3O^+ \quad (1)$$

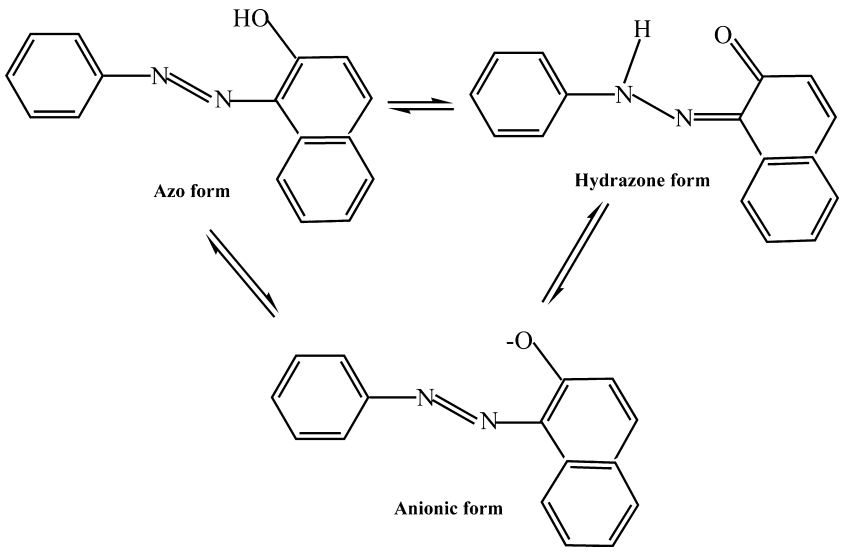

Fig. 1. Azo–hydrazo tautomeric and anionic forms of 1-phenylazo-2-napthol.

$$e^-_{aq} + N_2O + H2O \Rightarrow {}^\bullet OH + OH^- + N_2 \quad (2)$$

$$^\bullet OH + OH^- \rightleftharpoons O^{\bullet -} + H_2 \qquad Op K_a = 11.85 \quad (3)$$

3.3. High performance liquid chromatography (HPLC) and gas chromatography–mass spectrometry (GC/MS)

The HPLC and GC/MS analysis were carried out with three samples of dye solution at natural pH (a) un-irradiated as control (b) N_2O saturated (c) N_2-purged with added 0.2 mol dm^{-3} *tert*-butanol to remove the $^\bullet OH$ radicals. In case of HPLC analysis, air saturated and irradiated dye solution also had been analysed. Samples (b) and (c) were irradiated with ~4 kGy for GC/MS and 6 kGy for HPLC analysis, respectively. These samples were filtered and injected to HPLC. For GC/MS analysis, samples were lyophilized and extracted with chloroform followed by injection into GC/MS. For detailed methods of HPLC and GC/MS analysis see Supporting information.

3.4. Toxicity of the products: MTT assay

Chinese hamster ovary (CHO) cells suspended in DMEM medium with 10% fetal calf serum were seeded into 96 well plate at a density of 2×10^3 cells/well and incubated at 37 °C in 5% CO_2 humidified atmosphere. After the cells were attached (12–16 h), they were treated with increasing concentrations of test compounds for 24 h and cell viability was determined by a colorimetric MTT assay as described previously [36], for detail see Supporting information.

4. Results and discussion

The test dye being completely insoluble in water, the presence of the dye molecules would be restricted in the micelles only. The solubility of the dye in TX-100 micelle is confirmed from the absorption spectra of the dye in an optically clear solution, which also exhibits emission at 595 nm (Fig. S1). It should be mentioned here that the dye does not show any emission in acetonitrile–water mixture, whereas, in TX -100 it fluoresces, which might be due to decrease of the non-radiative pathways in the restricted micellar environment.

4.1. Determination of pK_a

The selected azo dye having hydroxyl group at ortho position to the azo bond exists in azo–hydrazone tautomeric forms. At a pH lower than the pK_a both the tautomers exist in equilibrium, with hydrazone being the dominating form [19,37–40], whereas at pH higher than pK_a the deprotonated azo form dominates. With the increase in pH of the solution (Fig. S2), the peak positions remain the same, (at 485 nm for the hydrazone form and a shoulder at 415 nm indicating the presence of azo tautomer) [40]. However, decrease in absorption for both the forms is observed with the increase in pH. The pK_a calculated from the inflexion point of pH vs. absorbance plot at 485 nm (inset of Fig. S2), was found to be 11.59, which is higher than other H-acids and this is attributed to the formation of a six membered ring through hydrogen bonding between the H atom of the naphthol ring and the N atom bound to the benzene ring [39,40]. Above pK_a, the single peak at 438 nm refers to the existence of azo form solely with the deprotonated phenol group.

4.2. Steady state gamma radiolysis

In general, irradiation experiments were carried out in de-aerated or N_2O-saturated solution to selectively create reducing or oxidizing conditions. For each of the experiments, appropriate solution of the dye was irradiated in Co-60 gamma chamber and the percentage of decolouration (Fig. 2) at 485 nm in the UV-visible spectra was plotted against the corresponding imparted dose.

Further, G (-dye) were calculated at each of the specified conditions and shown in Table 1. It can be seen from the table that the extent of degradation of the dye in oxidizing conditions are greater than those in reducing conditions both in acetonitrile–water and in TX-100 medium. Secondly, the degradation is greater in TX-100 medium than that in acetonitrile solution, which arises due to the

Table 1
The extent of degradation of the dye under various chemical conditions.

Conditions	G(-dye), molecules/100 eV
$OH^\bullet$ in Tx-100 (pH 7)	2.3
e^-_{aq} in Tx-100 (pH 7)	1.16
$H^\bullet$ in Tx-100 (pH 2)	0.5
Aerated in Tx-100 (pH 7)	0.614
$OH^\bullet$ in ACN (pH 7)	0.301
$OH^\bullet$ in ACN (pH 12.7)	0.536
e^-_{aq} in ACN (pH 7)	0.272
e^-_{aq} in ACN (pH 12.7)	0.391
Aerated in ACN (pH 7)	0.13
Aerated in ACN (pH 12.7)	0.182
Persulphate in ACN	0.294

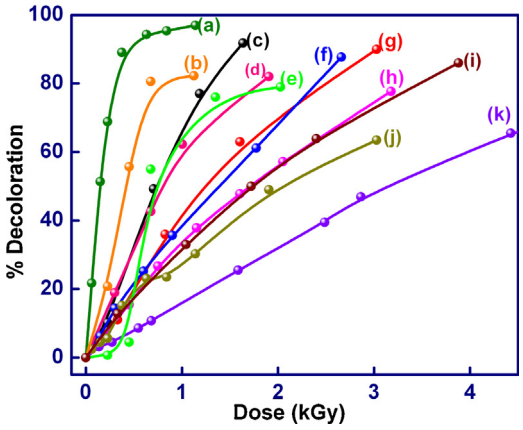

Fig. 2. Percent decolouration of 10^{-4} mol dm^{-3} dye under different conditions: (a) •OH in TX-100, pH 7 (b) e^-_{aq} in TX-100, pH 7 (c) •OH in 34% acetonitrile, pH 12.7 (d) e^-_{aq} in 34% acetonitrile, pH 12.7 (e) air saturated in TX-100, pH 7 (f) •OH in 34% acetonitrile, pH 7 (g) e^-_{aq} in 34% acetonitrile, pH 7 (h) air saturated in 34% acetonitrile, pH 12.7 (i) potassium persulphate in 34% acetonitrile (j) e^-_{aq} in TX-100, pH 2 (k) air saturated in 34% acetonitrile, pH 7.

confinement of the dye in micellar phase. In air saturated solutions, all the reactive species OH•, e^-_{aq}, H•, $O_2^{\bullet-}$, HO_2• are present. Under this reaction condition hydroxyl radicals react with the dye molecule whereas, the hydrated electrons react with O_2 and with dye competitively. Thus, it may be noted that under this condition and at a dose lower than 0.5 kGy (Fig. 2, curve e), decolouration is negligible. In presence of O_2, most of the H-atoms are scavenged and produces perhydroxyl radicals ($H^\bullet + O_2 = HO_2^\bullet$). At lower pH, the HO_2• radicals dominate whereas, at higher pH 12.7, $O_2^{\bullet-}$ radical is the predominant species [19].

Higher G (-dye) at pH 12.7 is due to the reaction of superoxide radical anion in addition to the OH•/$O^{\bullet-}$ radical induced degradation. Thus, at a dose of 3 kGy, the extents of decolouration are ~40% and 70% at pH 7.0 and 12.7, respectively (Fig. 2). The results also show that the HO_2• radical present at neutral pH of the solution, is not sufficiently strong oxidizing agent to cause any change in the dye. The G (-dye) is considerably lower in acetonitrile–water mixture. This is because a large number of radicals generated from water are facing acetonitrile, which is in higher proportion as compared to 10^{-4} mol dm^{-3} dye.

The hydroxyl radicals react with acetonitrile and the dye with bimolecular rate constants of 1.8×107 dm^3 mol^{-1} s^{-1} [41] and 5×10^9 dm^3 mol^{-1} s^{-1} [present work, see Table S1], respectively. Thus, considering the concentrations of acetonitrile and dye, it is clear that only 10% of the total dye could face the hydroxyl radicals and this is reflected in the lower decolouration of the dye under this reaction condition. Further, we did not notice any reaction of the acetonitrile radicals (produced via reaction of •OH radical) with the dye. While carrying out the degradation under the similar conditions but using a micellar medium, G (-dye) has been seen to be increased by around 5 times in reducing condition and 8 times in oxidising conditions as compared to that in aqueous acetonitrile mixture. Higher degradation in TX-100 micelle is due to the better trapping of the dye within the surfactant. The azo group being electron deficient in nature, the hydrated electrons attack these positions resulting in the degradation of the dye [42]. In a situation where e^-_{aq} is the only species, degradation at pH 12.7 is higher than that at pH 7, which further supports the dominance of azo form at higher pH.

Recently, dye degradation using sulphate radicals has also gained considerable importance. The degradation of dyes and organic contaminants by sulfate radicals ($SO_4^{\bullet-}$) at a near diffusion-controlled rate (10^9 dm^3 mol^{-1} s^{-1}) has been reported [43,44]. Thus, we intended to study the decolouration of the dye in the presence of $SO_4^{\bullet-}$ by gamma radiolysis. Potassium persulphate (1×10^{-3} mol dm^{-3}) in presence of 0.2 mol dm^{-3} *tert*-butanol produces $SO_4^{\bullet-}$ radical by reacting with hydrated electrons.

$$S_2O_8^{2-} + e^-_{aq} \rightarrow SO_4^{\bullet-} + SO_4^{2-} \quad (4)$$

Reaction of $SO_4^{\bullet-}$ radical causes decrease in absorbance, which follows a linear relation with dose (Figure not shown). The G (-dye) in presence of persulphate is 0.294, whereas in presence of e^-_{aq} it is 0.272. It indicates that the oxidation of the dye causes more degradation than the reduction process in aqueou–organic solvent.

4.3. Identification of products

4.3.1. HPLC and GC/MS analysis

HPLC Chromatograms [Fig. S3] obtained from four samples containing dye solution in TX-100 as (a) unirradiated (control) (b) air-saturated (c) N_2O-saturated (d) N_2 purged with added *tert*-butanol, were analysed quantitatively. Complete breakdown in samples (c), (d) and partial degradation in sample (b) were evident. Presence of two peaks at 3.25 min (57%) and 3.43 min (33%) were due to the existence of two tautomers of the dye in sample (a) [Fig. S3 (a)]. In sample (c), the appearance of two new major peaks at 31.5 min and 35 min demonstrated the complete breakdown of the dye by forming 44.5% and 44.6% products, respectively [Fig. S3 (c)]. Under reductive condition as in case of sample (d) same peaks appeared but with different concentrations of the products while comparing with the oxidizing conditions. From the chromatogram [Fig. S3 (d)] it was revealed that the peaks at 35 and 31.5 min were due to the formation of 74% and 10% products, respectively. Thus, both the oxidizing and reducing conditions in TX-100 micelle produced same products. Under air saturated condition [Fig. S3 (b)], retention of peaks of the original dye, indicated incomplete degradation. For further confirmation GC/MS analysis has been carried out. The products formed under oxidising and reducing conditions were identified and detailed in Table 2.

According to the literature, under reductive conditions, the hydrated electron cleaves the azo bond resulting in the formation of aniline and amino-naphthol as the major products, but the relative instability of amino-naphthol leads to the formation of further degraded products, like 1-naphthylamine, 2-naphthol and

Table 2
Products obtained from GC/MS analysis.

Peak no.	Retention time (min)	Majorfragment m/z	Otherfragments m/z	Calculated mass	Compound	Condition
1.	24.75	147	130,115,92	148	1,2,3,4-Tetrahydro-2-naphthol	e^-_{aq} in TX-100
2.	25.35	145	115,114,113,105	144	2-Naphthol	e^-_{aq} in TX-100
3.	26.14	93	94,66,67	93	Aniline	e^-_{aq} in TX-100
4.	27.00	99	70,56,43	98	Cyclohexylamine	e^-_{aq} and •OH in TX-100
5.	32.63	177	148,131,117	176	1,3-Dimethyl 1,2,3,4 tetra hydro-2-naphthol	e^-_{aq} and •OH in TX-100
6.	32.8	144	142,120,115	144	1-Naphthylamine	e^-_{aq} and •OH in TX-100
7.	36.87	135	134,120,119,107,9177,51,41	135	2,4,6-Trimethylaniline	e^-_{aq} and •OH in TX-100
8.	46.8	149	135,134	149	2,3,5,6-Tetramethylaniline	e^-_{aq} and •OH in TX-100

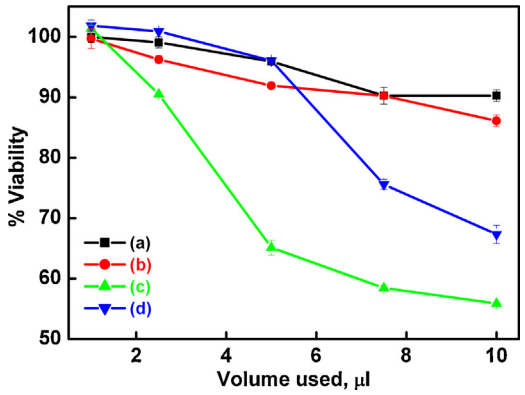

Fig. 3. The cytotoxic effects of increasing concentrations of (a) un-irradiated DMSO, (b) irradiated DMSO, (c) un-irradiated dye solution (d) irradiated dye solution, in CHO cells as determined by the MTT assay. Values are mean ± SEM of three experiments.

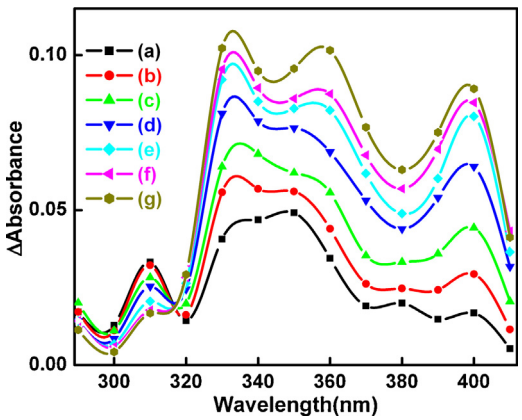

Fig. 4. Transient absorption spectra obtained from a N_2-purged aqueous solution containing 10^{-4} mol dm^{-3} dye, 10^{-2} mol dm^{-3} TX-100 and 0.2 mol dm^{-3} *tert*-butanol, pH 7. (a) 1 μs (b) 2.5 μs (c) 5 μs (d) 10 μs (e) 15 μs (f) 20 μs (g) 42 μs after the electron pulse.

1,2,3,4-tetrahydro 2-naphthol [45]. In the chromatogram obtained from GC/MS analysis, we could confirm the presence of aniline from the peak at 26.14 min. However, 1-amino-2-naphthol could not be detected in the present experiment, probably due to its low volatility or instability. The peaks at 24.75, 25.35 and 32.8 min were identified as 1,2,3,4-tetrahydro 2-naphthol, 2-naphthol and 1-naphthylamine, respectively, which confirmed the dissociation of the azo bond. Furthermore, three methyl substituted products viz. 1,3-dimethyl-1,2,3,4 tetrahydro-2-naphthol, 2,4,6-trimethylaniline and 2,3,5,6-tetramethylaniline were also detected at R_t 32.63, 36.87 and 46.8 min, respectively under both oxidizing and reducing conditions. As the degradation studies have been carried out in surfactant medium, the alkyl radicals produced from TX-100 probably adds to the aromatic rings (benzene and naphthyl) forming alkyl substituted products as shown in Table 2. Cyclohexylamine could also be identified for the first time as one of the degraded products under both the conditions. Earlier, Greenfield has reported the hydrogenation of aniline to cyclohexylamine by platinum metal catalyst [46], however, the mechanism of its formation in our present study demands further investigation.

4.4. Toxicity

The cytotoxic effects of irradiated and un-irradiated dye in CHO cells as shown in Fig. 3, it is clear that the un-irradiated dye led to an increase in cytotoxicity in a concentration dependent manner. At the highest test concentration (5 μM) of un-irradiated dye, the viability of CHO cells was reduced to 55%. The irradiation of dye significantly reduced its cytotoxic effect in CHO cells. For example, the irradiated dye exhibited the viability of 67% at the highest test concentration (5 μM). The vehicle or DMSO showed negligible cytotoxicity both under irradiated and un-irradiated conditions. The surfactant TX-100 itself being toxic towards the cell, the cytotoxic experiments were carried out in DMSO medium.

4.5. Mechanism of degradation

4.5.1. Reaction of hydrated electron

At pH 7, the dye primarily remains in its hydrazone tautomer with a negligible amount of azo form. Earlier studies on the electron density calculation of napthol dyes namely acid orange and its derivatives showed that the nucleophilic reactions occur at the nitrogen atom bound to the naphthalene ring [19,38,42,47]. Triton-X 100 being very less reactive with e^-_{aq}, it is possible to study its sole reaction with the dye in this medium [48–50]. The reaction of e^-_{aq} with the dye produces transient spectra as shown in Fig. 4. Immediately after the reaction, two absorption peaks at 310 nm and 340 nm in the spectrum can be attributed to the hydrazyl radical produced due to the electron addition to the nitrogen atom attached to the naphthalene ring followed by protonation. The bimolecular rate constant for the growth of the 340 nm band was 2.5×10^{10} dm^3 mol^{-1} s^{-1}.

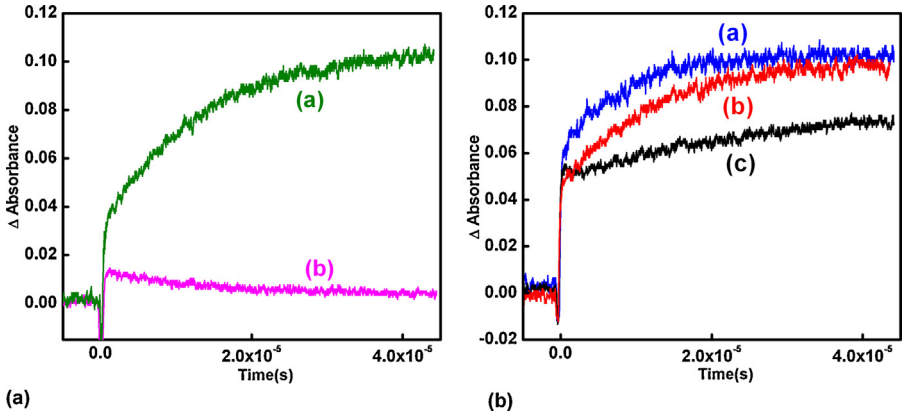

Fig. 5. (a) Kinetic traces showing the decay of hydrazyl radical and formation of the adduct at (b) 300 nm and (a) 360 nm, respectively in the reaction of hydrated electrons with the dye. (a) Kinetic traces obtained from the reaction of hydrated electron with the dye (in 10^{-2} mol dm^{-3} TX-100) at 350 nm showing the variation in rate of formation at different concentrations of the dye (a) 2×10^{-4} mol dm^{-3}, (b) 10^{-4} mol dm^{-3}, (c) 0.5×10^{-4} mol dm^{-3}.

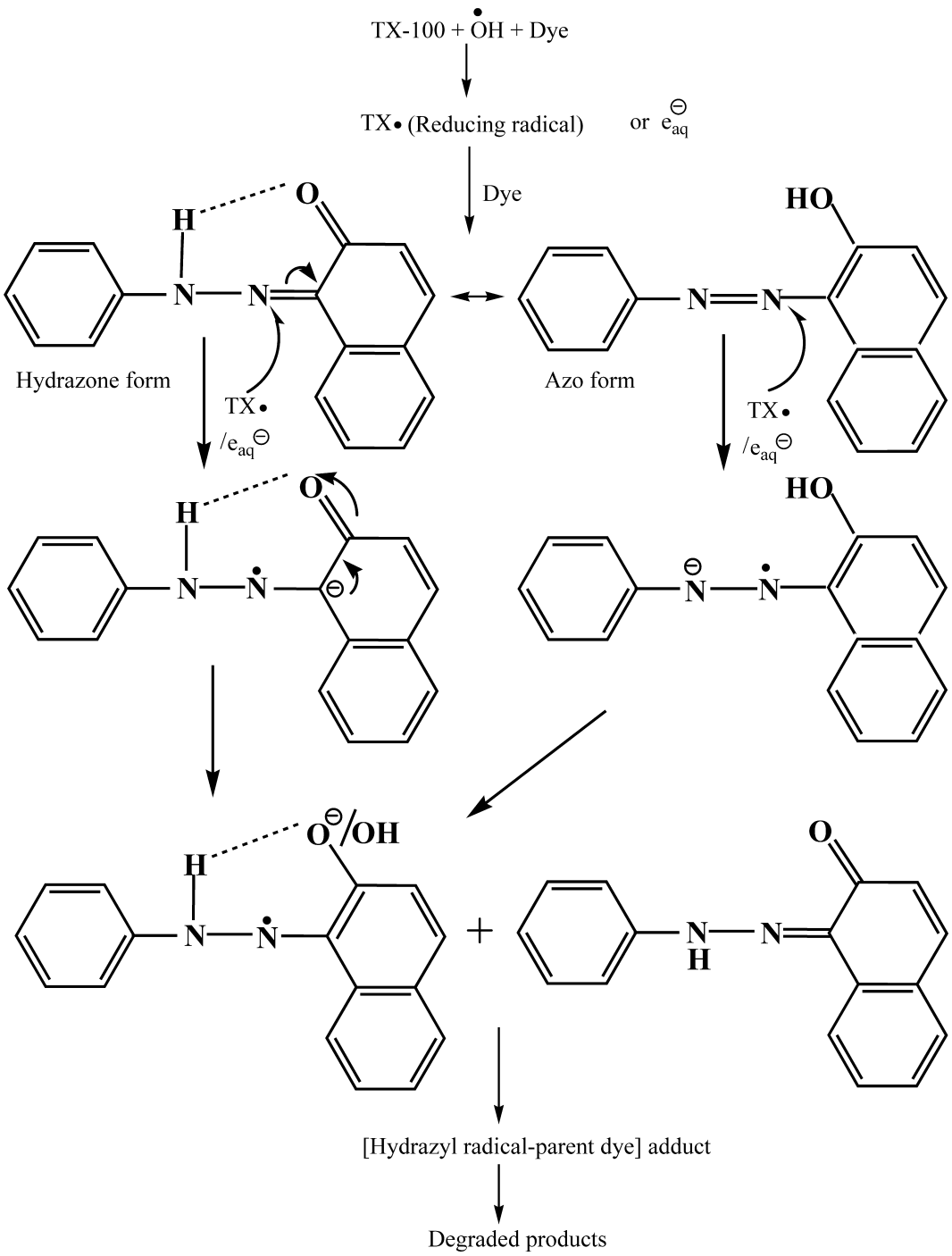

Fig. 6. Mechanistic pathway for reduction reaction of the azo dye showing the formation of hydrazyl radical-parent adduct.

The protonation step being instant, the demarcation between the two species could not be achieved. This is in close agreement with earlier studies on hydrated electron reaction with azo dyes [19,41,51]. With the progress in time, absorption at 310 nm decreases with emergence of three new peaks at 330, 360 and 390 nm. Fig. 5(a) shows the simultaneous decay and formation at 20 μs time scale. Absorbance at 360 and 390nm decay at the same rate which show that these are due to the same species. As has been mentioned earlier, in many cases of the reaction of these dyes, overlapping absorptions of intermediate species, products and the parent causes difficulties in assigning absorption band for individual species. Most interestingly it has been observed that the growth of 360 nm and 390 nm band is dependent on concentration of the parent molecule. Fig. 5(b) shows the effect of dye concentration on the growth of absorption at 360 and 390 nm. This result suggests that the hydrazyl radical interacts with the parent to form an adduct. At higher concentrations only two step growth is visible, while at lower concentration both the decay of hydrazyl radical and growth of the adduct dimer can clearly be observed. The general mechanism for the reaction of e^{-}_{aq} with napthol dyes follows a disproportionation reaction [21,51] of the hydrazyl radicals. In the present case, we have not observed any signature of dose dependency, which may be due to overlapping absorptions of intermediates as well as products and parent molecule. However,

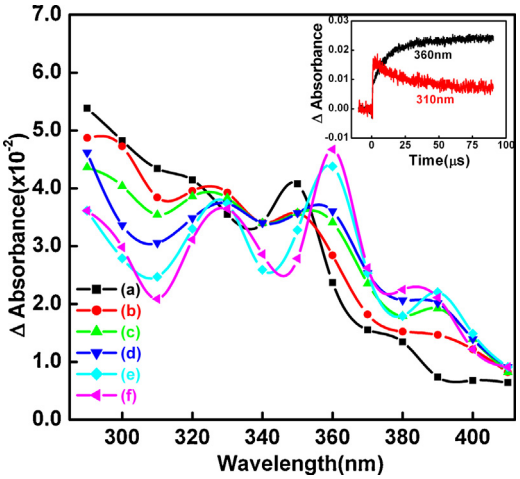

Fig. 7. Transient absorption spectra obtained from an N_2O-saturated aqueous solution containing 10^{-4} mol dm^{-3} dye and 10^{-2} mol dm^{-3} TX-100, dose of 38 Gy/pulse, pH 7 (a) 1.2 μs (b) 6 μs (c) 15 μs (d) 25 μs (e) 55 μs (f) 88 μs after the electron pulse. Inset: Kinetic traces showing the decay of the transient at 310 nm and formation of the adduct at 360 nm, respectively.

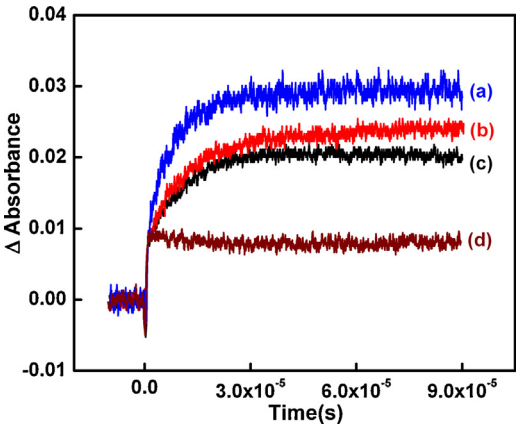

Fig. 8. Kinetic traces for hydroxyl radical reaction with the dye (in 10^{-2} mol dm^{-3} TX-100) at 360 nm showing the increase in rate of formation with increase in concentration: (a) 2×10^{-4} mol dm^{-3}, (b) 1×10^{-4} mol dm^{-3}, (c) 0.5×10^{-4} mol dm^{-3} (d) 0.3×10^{-4} mol dm^{-3}.

disproportionation cannot be ruled out. Interestingly, the adduct formation between hydrazyl radical and the parent molecule was observed in case of azo benzene derivatives in alcohol [52]. However, in case of naphthol or other dyes, this type of associated intermediate has not been directly attested in aqueous solution so far. Of course, Zielonka et al. [53] by matrix relaxation technique had proposed such possibility. In the present case, the said adduct was possible to observe because of the close proximity of the dye molecules in a confined micellar volume. At lower dye concentration, each micelle might not contain more than one dye; and thus, both adduct formation and disproportionation becomes very slow to detect at the time scale mentioned. Following these arguments, we now propose the mechanism of hydrated electron reaction with the azo-napthol dye [Fig. 6].

4.5.2. Hydroxyl radical reaction: surfactant derived radical and its interaction with the dye

In contrast to the hydrated electrons, the hydroxyl radical reacts very fast with TX-100 [48,49] producing different radicals including cyclohexadienyl and other aliphatic radicals. Thus, the concentration of the dye was chosen in such a way that all the OH radicals react with TX-100 in the first step, and then we have followed the reaction of the surfactant radicals with the dye. In general, the mechanism of oxidation of water soluble azo dyes with the similar molecular structure known from earlier literature is the following. $^{\bullet}$OH radical adds to the phenyl ring producing a hydroxycyclohexadienyl radical of the dye [23,25,42]. This radical is known to undergo disproportionation and dimerization with another dye radical. However, in the present case, we expect a different mechanism for the OH radical induced degradation of the dye in presence of large concentration of TX-100. In fact, we have recorded the transient absorption spectra obtained in the reaction of hydroxyl radical with TX-100 alone (Fig. S4). The spectrum shows a featureless broad absorption in the range of 300–400 nm region, which matches well with that reported earlier [48,49]. This band was attributed to cyclohexadienyl radical, while possible aliphatic radicals generated from TX-100 could not be detected in this case, as these absorb in the UV region below the detection limit of our optical set up.

Even in case of 0.1×10^{-3} mol dm^{-3} dye been added to 10×10^{-3} mol dm^{-3} TX-100, at the end of the electron pulse, the transient spectra shows similar characteristics of the TX-100 derived radicals with a broad peak near 300 nm and shoulder at 340–350 nm (Fig. 7). But at 15 μs, the peak at 300 nm has significantly decreased indicating the decay of the TX-100 radical, while absorptions at 360 and 385 nm started increasing. Absorptions at these wavelengths become more prominent as peaks appear at around 90 μs. It is to be mentioned that these peaks are absent in neat TX-100 both in the present work and in earlier literature. This result shows that in the second step, the dye radicals are produced as a consequence of an interaction between the dye and the TX-100 radical.

The concentrations dependent study reveals the dimer adduct formation between the dye radicals and parent dye (Fig. 8). The most important point at this stage is to identify the type of the reaction; i.e. oxidation or reduction. Simply one needs to know whether the TX-100 radical is oxidizing or reducing in nature.

It is known that methyl viologen (MV^{2+}) is an efficient electron acceptor and is converted to $MV^{\bullet+}$ in a reducing condition, which shows characteristic absorption at 390 and 605 nm. In an N_2O-saturated solution containing TX-100 and MV^{2+}, a clear signal of $MV^{\bullet+}$ could be observed both at 390 and 605 nm (Fig. S5) after the electron pulse. This result confirms the reducing nature of the TX-100 radicals. When MV^{2+} has been replaced by a well-established electron donor ABTS [2,2′-azino-bis (3-ethylbenzothiazoline-6-sulphonic acid), no signature of ABTS radical formation could be observed, confirming the absence of any oxidizing radical in the irradiated TX-100 solution. Thus, it is clear that a reduced species of the dye is produced in its reaction with TX-100 radical. It is now clear that both the reactions of the dye with hydroxyl radicals and the hydrated electrons proceed through reductive mechanism, composed in Fig. 6. The mechanism, however, predicts higher degradation of the dye than observed. This provides further scope for future research in this direction.

5. Conclusions

We have provided a conclusive and direct evidence for the adduct formation between the hydrazyl radical and the unreacted dye molecule. In earlier reports [19], it had been shown that the hydrazyl radical either dimerizes or disproportionates. In contrast to these reports, we have proposed that adduct formation is favoured due to close proximity of the hydrazyl radical and the hydrophobic dye molecules in a single micelle. Further, the importance of surfactants on the degradation of organic compounds [54] had been mentioned earlier. However, such studies involving the dyes are feebly available in literature. Only recently, a simulated

mixture of textile waste treated by gamma radiolysis [32] has been reported, which did not focus on the interaction of surfactant derived radical with the dyes. We have shown here that the surfactants play important role in the efficiency and mechanism for degradation of the dye, and maximum degradation is achieved in the hydroxyl radical reaction with the dye in surfactant medium. In general, advanced oxidation processes, such as UV/H_2O_2 oxidation, Fenton process, photoelectrocatalytic oxidation on oxide surfaces, employ hydroxyl radicals for degradation and mineralization of azo dyes. We have clearly demonstrated that hydroxyl radical; a strong oxidizing species produces intermediates of surfactant, which are reducing in nature. These surfactant radicals cause further degradation of the azo dyes via reductive pathway. Thus, the complete reaction scheme, the products and their toxicity behaviour would be different in the two cases, with actual textile-effluent and individual dye solutions, treated via advanced oxidation process. This point warns for future research that proper care is necessary prior to selection of a process for the degradation of textile waste especially via advanced oxidation process, which employs hydroxyl radicals.

Acknowledgements

The authors thank Dr D.K. Palit, Head, Radiation & Photochemistry Division and Dr K. Indira Priyadarsini, Head, Radiation Chemistry and Biology Section, for their constant encouragement and support.

Appendix A. Supplementary data

Supplementary data associated with this article can be found, in the online version, at http://dx.doi.org/10.1016/j.jhazmat.2015.04.084

References

[1] L. Zhang, J.M. Cole, P.G. Waddell, K.S. Low, X. Liu, Relating electron donor and carboxylic acid anchoring substitution effects in azo dyes to dye-sensitized solar cell performance, ACS Sustain. Chem. Eng. 1 (2013) 1440–1452.
[2] A. Gottlieb, C. Shaw, A. Smith, A. Wheatley, S. Forsythe, The toxicity of textile reactive azo dyes after hydrolysis and decolourisation, J. Biotechnol. 101 (2003) 49–56.
[3] D. Prato-Garcia, F.J. Cervantes, G. Buitrón, Azo dye decolorization assisted by chemical and biogenic sulphide, J. Hazard. Mater. 250–251 (2013) 462–468.
[4] B. Jiang, J. Zheng, Q. Liu, M. Wu, Degradation of azo dye using non-thermal plasma advanced oxidation process in a circulatory airtight reactor system, Chem. Eng. J. 204–206 (2012) 32–39.
[5] S. Haji, B. Benstaali, N. Al-Bastaki, Degradation of methyl orange by UV/H_2O_2 advanced oxidation process, Chem. Eng. J. 168 (2011) 134–139.
[6] M.S. Lucas, J.A. Peres, Decolorization of the azo dye reactive black 5 by Fenton and photo-Fenton oxidation, Dyes Pigm. 71 (2006) 236–244.
[7] R.L. de Oliveira, M.A. Anderson, G. de Aragão Umbuzeiro, G.J. Zocolo, M.V.B. Zanoni, Assessment of by-products of chlorination and photoelectrocatalytic chlorination of an azo dye, J. Hazard. Mater. 205–206 (2012) 1–9.
[8] R.V. Khandare, A.N. Kabra, M.B. Kurade, S.P. Govindwar, Phytoremediation potential of *Portulaca grandiflora* Hook. (Moss-Rose) in degrading a sulfonated diazo reactive dye navy blue HE2R (Reactive Blue 172), Bioresour. Technol. 102 (2011) 6774–6777.
[9] S. Athalathil, F. Stüber, C. Bengoa, J. Font, A. Fortuny, A. Fabregat, Characterization and performance of carbonaceous materials obtained from exhausted sludges for the anaerobic biodecolorization of the azo dye Acid Orange II, J. Hazard. Mater. 267 (2014) 21–30.
[10] Md.M. Haque, W.T. Smith, D.K.Y. Wong, Conducting polypyrrole films as a potential tool for electrochemical treatment of azo dyes in textile wastewaters, J. Hazard. Mater. 283 (2015) 164–170.
[11] N. Raghavan, S. Thangavel, G. Venugopal, Enhanced photocatalytic degradation of methylene blue by reduced grapheme oxide/titaniumdioxide/zincoxide ternary nanocomposites, Mater. Sci. Semicond. Process. 27 (2014) 212–219.
[12] S. Thangavel, G. Venugopal, S.J. Kim, Enhanced photocatalytic efficacy of organic dyes using β-tin tungstate-reduced graphene oxide nanocomposites, Mater. Chem. Phys. 145 (2014) 108–115.
[13] H.T. Chandran, S. Thangavel, C.V. Jipsa, G. Venugopal, Study on inorganic oxidants assisted sonocatalytic degradation of Resazurin dye in presence of β-$SnWO_4$ nanoparticles, Mater. Sci. Semicond. Process. 30 (2015) 321–329.
[14] S. Thangavel, N. Raghavan, G. Kadarkarai, S.J. Kim, G. Venugopal, Graphene-oxide (GO) – Fe^{3+} hybrid nanosheets with effective sonocatalytic degradation of Reactive Red 120 and study of their kinetics mechanism, Ultrason. Sonochem. 24 (2015) 123–131.
[15] E. Kusvuran, O. Gulnaz, S. Irmak, O.M. Atanur, H.I. Yavuz, O. Erbatur, Comparison of several advanced oxidation processes for the decolorization of Reactive Red 120 azo dye in aqueous solution, J. Hazard. Mater. B 109 (2004) 85–93.
[16] B.P. Chaplin, Critical review of electrochemical advanced oxidation processes for water treatment applications, Environ. Sci. Process. Impacts 16 (2014) 1182.
[17] T. Maezono, M. Tokumura, M. Sekine, Y. Kawase, Hydroxyl radical concentration profile in photo-Fenton oxidation process: generation and consumption of hydroxyl radicals during the discoloration of azo-dye Orange II, Chemosphere 82 (2011) 1422–1430.
[18] M.A. Rauf, S.S. Ashraf, Radiation induced degradation of dyes – an overview, J. Hazard. Mater. 166 (2009) 6–16.
[19] L. Wojnárovits, E. Takács, Irradiation treatment of azo dye containing wastewater: an overview, Radiat. Phys. Chem. 77 (2008) 225–244.
[20] E. Takács, L. Wojnárovits, T. Pálfi, Azo dye degradation by high-energy irradiation: kinetics and mechanism of destruction, Nukleonika 52 (2) (2007) 69–75.
[21] K.K. Sharma, B.S.M. Rao, H. Mohan, J.P. Mittal, J. Oakes, P. O' Neill, Free-radical-induced oxidation and reduction of 1-arylazo-2-naphthol dyes: A radiation chemical study, J. Phys. Chem. A 106 (2002) 2915–2923.
[22] E. Kusvuran, S. Irmak, H.I. Yavuz, A. Samil, O. Erbatur, Comparison of the treatment methods efficiency for decolorization and mineralization of Reactive Black 5 azo dye, J. Hazard. Mater. B 119 (2005) 109–116.
[23] L. Wojnárovits, T. Pálfi, E. Takács, S.S. Emmi, Reactivity differences of hydroxyl radicals and hydrated electrons in destructing azo dyes, Radiat. Phys. Chem. 74 (2005) 239–246.
[24] L. Wojnárovits, T. Pálfi, E. Takács, Kinetics and mechanism of azo dye destruction in advanced oxidation processes, Radiat. Phys. Chem. 76 (2007) 1497–1501.
[25] J. Paul, D.B. Naik, S. Sabharwal, High energy induced decoloration and mineralization of reactive red 120 dye in aqueous solution: a steady state and pulse radiolysis study, Radiat. Phys. Chem. 79 (2010) 770–776.
[26] J.J.F. Coen, A.T. Smith, L.P. Candeias, J. Oakes, New insights into mechanisms of dye degradation by one electron oxidation process, J. Chem. Soc. Perkin Trans. 2 (2001) 2125–2129.
[27] M. Stiborová, V. Martínek, H. Rýdlová, P. Hodek, E. Frei, Sudan I Is a potential carcinogen for humans: evidence for its metabolic activation and detoxication by human recombinant cytochrome P450 1A1 and liver microsomes, Cancer Res. 62 (2002) 5678–5684.
[28] L. Li, H.W. Gao, J.R. Ren, L. Chen, Y.C. Li, J.F. Zhao, H.P. Zhaoand, Y. Yuan, Binding of Sudan II and IV to lecithin liposomes and *E. coli* membranes insights into the toxicity of hydrophobic azo dyes, BMC Struct. Biol. 7 (2007) 16.
[29] M. Ma, X. Luo, B. Chen, S. Su, S. Yao, Simultaneous determination of water-soluble and fat-soluble synthetic colorants in foodstuff by high-performance liquid chromatography–diode array detection–electrospray mass spectrometry, J. Chromatogr. A 1103 (2006) 170–176.
[30] M. Tateo, F. Bononi, Fast determination of Sudan I by HPLC/APCI–MS in hot chilli spices, and oven-baked foods, J. Agric. Food Chem. 52 (2004) 655–658.
[31] H.Y. Lee, X. Song, H. Park, M.H. Baik, D. Lee, Torsionally responsive C3-symmetric azo dyes: azo–hydrazone tautomerism, conformational switching, and application for chemical sensing, J. Am. Chem. Soc. 132 (2010) 12133–12144.
[32] J.P. Guin, D.B. Naik, L. Bhardwaj, Y.K. Varshney, An insight into the effective advanced oxidation process for treatment of simulated textile dye waste water, RSC Adv. 4 (2014) 39941–39947.
[33] A. Reza, T. Bagha, K. Holmberg, Solubilization of hydrophobic dyes in surfactant solutions, Materials 6 (2013) 580–608.
[34] S.N. Guha, P.N. Moorthy, D.B. Naik, K.N. Rao, One-electron reduction of thionine studied by pulse radiolysis, Proc. Indian Acad. Sci. (ChemSci) 99 (1987) 261–271.
[35] G.V. Buxton, C.R. Stuart, Reevaluation of the thiocyanate dosimeter for pulse radiolysis, J. Chem. Soc. Faraday Trans. 91 (1995) 279–281.
[36] T. Mosmann, Rapid colorimetric assay for cellular growth and survival: application to proliferation and cytotoxicity assays, J. Immunol. Methods 65 (1983) 55–63.
[37] T. Hihara, Y. Okada, Z. Morita, Photo-oxidation of pyrazolinylazo dyes and analysis of reactivity as azo and hydrazine tautomers using semiempirical molecular orbital PM5 method, Dyes Pigm. 69 (2006) 151–176.
[38] T. Hihara, Y. Okada, Z. Morita, Reactivity of phenylazonaphthol sulfonates their estimation by semiempirical molecular orbital PM5 method, and the relation between their reactivity and azo–hydrazone tautomerism, Dyes Pigm. 59 (2003) 201–222.
[39] K. Bredereck, C. Schumacher, Structure reactivity correlations of azo reactive dyes based on H-acid. I. NMR chemical shift values pK_a values, dyes aggregation and dyeing behaviour, Dyes Pigm. 21 (1993) 23–43.
[40] J. Oakes, P. Gratton, Kinetic investigations of azo dye oxidation in aqueous media, J. Chem. Soc. Perkin Trans. 2 (1998) 1857–1864.
[41] A.J. Hynes, P.H. Wine, Kinetics and mechanism of the reaction of hydroxyl radicals with acetonitrile under atmospheric conditions, J. Phys. Chem. 95 (1991) 1232–1240.

[42] T. Pálfi, L. Wojnárovits, E. Takács, Mechanism of azo dye degradation in advanced oxidation processes: degradation of sulfanilic acid azochromotrop and its parent compounds in aqueous solution by ionizing radiation, Radiat. Phys. Chem. 80 (2011) 462–470.
[43] X. Chen, Z. Xue, Y. Yao, W. Wang, F. Zhu, C. Hong, Oxidation degradation of rhodamine B in aqueous by UV/$S_2O_8^{2-}$ treatment system, Int. J. Photoenergy 2012 (2012) 1–5.
[44] K.C. Huang, Z. Zhao, G.E. Hoag, A. Dahmani, P.A. Block, Degradation of volatile organic compounds with thermally activated persulfate oxidation, Chemosphere 61 (2005) 551–560.
[45] S.J. Zhang, H.Q. Yu, Q.R. Li, Radiolytic degradation of acid orange 7: a mechanistic study, Chemosphere 61 (2005) 1003–1011.
[46] H. Greenfield, Hydrogenation of aniline to cyclohexylamine with platinum metal catalysts, J. Org. Chem. 29 (1964) 3082–3084.
[47] A.S. Ozen, V. Aviyente, Modelling of oxidative degradation of azo dyes: a density functional theory study, J. Phys. Chem. A 107 (2003) 4898–4907.
[48] J. Perkowski, J. Mayer, L. Kos, Reactions of non-ionic surfactants triton X-*n* type, with OH radicals. A review, Fibres Text. East. Eur. 13 (2005) 81–85.
[49] J. Perkowski, J. Mayer, Pulse radiolysis of triton X-100 aqueous solution, J. Radioanal. Nucl. Chem. 141 (1990) 271–277.
[50] J. Perkowski, J. Mayer, Gamma radiolysis of triton X-100 aqueous solution, J. Radioanal. Nucl. Chem. 157 (1992) 27–36.
[51] K.K. Sharma, P.O. Neill, J. Oakes, S.N. Batchelor, B.S.M. Rao, One-electron oxidation and reduction of different tautomeric forms of azo dyes: a pulse radiolysis study, J. Phys. Chem. A 107 (2003) 7619–7628.
[52] L. Flamigni, S. Monti, Primary processes in the reduction of azo dyes in alchohols studied by pulse radiolysis, J. Phys. Chem. 89 (1985) 3702–3707.
[53] J. Zielonka, R. Podsiadly, M. Czerwinska, A. Sikora, J. Sokolowska, A. Marcinek, Color changes accompanying one-electron reduction and oxidation of the azo dyes, J. Photochem. Photobiol. A Chem. 163 (2004) 373–379.
[54] G. Zacheis, K. Gray, P.V. Kamat, Radiolytic reduction of hexachlorobenzene in surfactant solutions: a steady-state and pulse radiolysis study, Environ. Sci. Technol. 34 (2000) 3401–3407.